the length of a single chain, i.e., approximately one micrometer or less. Relevant to this is our finding that trapping of holes on the polymer chains themselves does not appear to occur.

Experimental

Oxygen saturated, dilute benzene solutions (corresponding to ca. 1 mM monomer units) of the polymers shown in Figure 1 were contained in a microwave cell of internal dimensions $3.5 \times 7.1 \times 24$ mm^3. The solutions were irradiated with 5 or 10 ns pulses of 3 MeV electrons from a Van de Graaff accelerator with a total absorbed dose per pulse, D, of approximately 1×10^4 J/m^3 which was accurately measured for each experiment. This resulted initially in the formation of a uniform concentration of ca. 0.1 μM of excess electrons and benzene radical cations. The resulting change in the conductivity of the solution was measured as the change in the power of microwaves (26–38 GHz) reflected by the cell. Using only a single pulse the radiation-induced conductivity could be monitored from 10 ns to 1 ms using a pseudo-logarithmic time-base. The experimental methodology and data reduction procedures have been described in detail previously [4,5].

Received: September 21, 2001
Final version: November 2, 2001

[1] G. E. Moore, *Electron. Mag.* **1965**, *38*, 114.
[2] K. Shinsaka, G. R. Freeman, *Can. J. Chem.* **1974**, *52*, 3495.
[3] S. S.-S. Huang, G. R. Freeman, *J. Chem. Phys.* **1979**, *72*, 1989.
[4] P. P. Infelta, M. P. de Haas, J. M. Warman, *Radiat. Phys. Chem.* **1977**, *10*, 353.
[5] J. M. Warman, M. P. de Haas, in *Pulse Radiolysis* (Ed: Y. Tabata), CRC Press, Boca Raton, FL **1991**, Ch. 6.
[6] R. J. O. M. Hoofman, M. P. de Haas, L. D. A. Siebbeles, J. M. Warman, *Nature* **1998**, *392*, 54.
[7] W. F.Schmidt, A. O. Allen, *J. Phys. Chem.* **1968**, *72*, 3730.
[8] N. Gee, G. R. Freeman, *Can. J. Chem.* **1992**, *70*, 1618.
[9] A. O. Allen, M. P. de Haas, A. Hummel, *J. Chem. Phys.* **1976**, *64*, 2587.
[10] R. M. Noyes, in *Progress in Reaction Kinetics*, Vol. 1 (Ed: G. Porter), Pergamon, London **1961**, Ch. 5.
[11] R. D. Miller, J. Michl, *Chem. Rev.* **1989**, *89*, 1359.
[12] H. Teramae, K. Takeda, *J. Am. Chem. Soc.* **1989**, *111*, 1281.
[13] J. W. Mintmire, *Phys. Rev. B* **1989**, *39*, 13 350.
[14] G. P. van der Laan, M. P. de Haas, A. Hummel, H. Frey, M. Möller, *J. Phys. Chem.* **1996**, *100*, 5470.
[15] F. C. Grozema, P. T. van Duijnen, Y. A. Berlin, M. A. Ratner, L. D. A. Siebbeles, unpublished.
[16] H. Sirringhaus, P. J. Brown, R. H. Friend, M. M. Nielsen, K. Bechgaard, B. M. W. Langeveld-Voss, A. J. H. Splering, R. A. J. Janssen, E. W. Meijer, P. Herwig, D. M. de Leeuw, *Nature* **1999**, *401*, 685.
[17] G. Lieser, M. Oda, T. Miteva, A. Meisel, H.-G. Nothofer, U. Scherf, *Macromolecules* **2000**, *33*, 4490.
[18] M. Redecker, D. D. C. Bradley, M. Inbasekaran, E. P. Woo, *Appl. Phys. Lett.* **1999**, *74*, 1400.
[19] H. Sirringhaus, R. J. Wilson, R. H. Friend, M. Inbasekaran, W. Wu, E. P. Woo, M. Grell, D. D. C. Bradley, *Appl. Phys. Lett.* **2000**, *77*, 406.
[20] M. Redecker, D. D. C. Bradley, M. Inbasekaran, E. P. Woo, *Appl. Phys. Lett.* **1998**, *73*, 1565.
[21] D. Hertel, U. Scherf, H. Bässler, *Adv. Mater.* **1998**, *10*, 1119.
[22] D. Hertel, H. Bässler, U. Scherf, H. H. Hörhold, *J. Chem. Phys.* **1999**, *110*, 9214.
[23] Y. Kunimi, S. Seki, S. Tagawa, *Solid State Commun.* **2000**, *114*, 469.
[24] S. Seki, Y. Yoshida, S. Tagawa, K. Asai, K. Ishigure, K. Furukawa, M. Fujiki, N. Matsumoto, *Philos. Mag. B* **1999**, *79*, 1631.

Arrays of Magnetic Nanoparticles Patterned via "Dip-Pen" Nanolithography**

By *Xiaogang Liu*, *Lei Fu*, *Seunghun Hong*, *Vinayak P. Dravid*,* and *Chad A. Mirkin**

There has been considerable recent interest in developing methods for patterning ultrafine magnetic particles because of their potential technological applications in molecular electronics, magnetic storage devices, and biosensors.[1–4] Advances in nanofabrication technology and lithographic methods have made it possible to: 1) develop new magnetic storage devices with higher storage densities and faster speeds, 2) prepare arrays of interactive magnetic nanoparticles with precisely controlled magnetization orientation and interparticle spacing, and 3) obtain a better understanding of the relationship between magnetic feature size and magnetism. A variety of techniques, including electron-beam lithography,[5] microcontact printing,[6] scanning tunneling microscope lithography,[7] electrochemical etching, and electrodeposition,[8] have been used to fabricate arrays of magnetic structures on semiconductor substrates with dimensions in the sub-100 nm to micrometer length scale. However, there are some inherent limitations associated with these methods including the need for complex instrumentation, costly fabrication procedures, and complex and time-consuming processing steps. Herein, we present a new and straightforward strategy, based upon dip-pen nanolithography (DPN), for preparing nanometer-scale magnetic structures with precise feature size control.

DPN allows one to transport molecules to a surface, much like a macroscopic dip-pen transfers ink to paper, but with the resolution of a conventional atomic force microscope (AFM),[9–15] Scheme 1. Chemisorption of an ink (e.g., 16-mercaptohexadecanoic acid, MHA) onto the substrate leads to stable nanostructures, which can subsequently be used as templates to assemble different types of molecules or nanostructures of interest, including magnetic nanoparticles and alkylamine-modified deoxyribonucleic acid (DNA).[15]

Magnetic iron oxide nanoparticles were prepared by the slow addition of an aqueous solution of ferrous chloride (2 g $FeCl_2$ in 5 mL 2 M HCl) to an aqueous solution of ferric chloride (3.2 g $FeCl_3$ in 20 mL 2 M HCl) at room temperature.[16]

[*] Prof. C. A. Mirkin, X. Liu, Dr. S. Hong[+]
Department of Chemistry and Center for Nanofabrication and Molecular Self-assembly
Northwestern University
2145 Sheridan Road, Evanston, IL 60208 (USA)
E-mail: camirkin@chem.northwestern.edu
Prof. V. P. Dravid, Dr. L. Fu
Department of Materials Science and Engineering
Northwestern University
2145 Sheridan Road, Evanston, IL 60208 (USA)
E-mail: v-dravid@northwestern.edu
[+] Present address: Department of Physics, Florida State University, Tallahassee, FL 32306-4350, USA.

[**] We acknowledge the AFOSR, DARPA, and NSF for support of this research.

 © WILEY-VCH Verlag GmbH, D-69469 Weinheim, 2002 0935-9648/02/0302-0231 $ 17.50+.50/0

ADVANCED MATERIALS

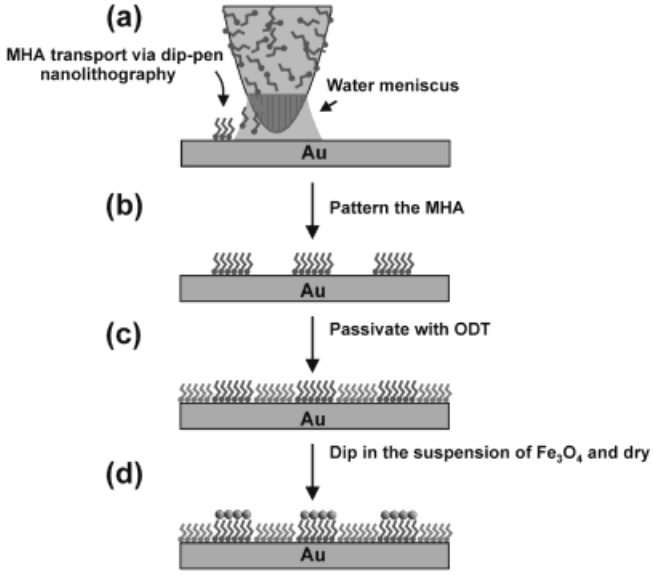

Scheme 1. Schematic representation of the procedure used to prepare magnetic nanostructures on a Au substrate.

The solution was stirred vigorously for 30 min, and then ammonium hydroxide (30 mL, 28 % NH_3 in water) was added dropwise to it, resulting in the concomitant formation of a precipitate. The precipitate was centrifuged, and the supernatant was decanted to afford the iron oxide particles (magnetite, Fe_3O_4). The particles were then mixed with a solution of tetramethylammonium hydroxide (20 mL, 25 wt.-% solution in water), which was used as a surfactant to stabilize the particles in an aqueous environment by repulsive double-layer interactions and to increase their affinity for negatively charged surfaces (e.g., deprotonated MHA). To ensure adequate dispersion of the magnetic particles, the solution was vigorously stirred prior to each pattern modification step (see below).

Transmission electron microscopy (TEM), Figure 1, shows that the magnetic particles are nearly spherical in shape and exhibit a size distribution from 4 to 16 nm. The mean particle size is 9.58 nm with a standard deviation of 2.53 nm. The surfactant coating on the surface of the magnetic particles was confirmed by thermogravimetric analysis (TGA) measurements, which show an 18 % weight loss over a temperature range of 150–360 °C. The weight loss was attributed to the desorption and evaporation of the surfactant from the particles.

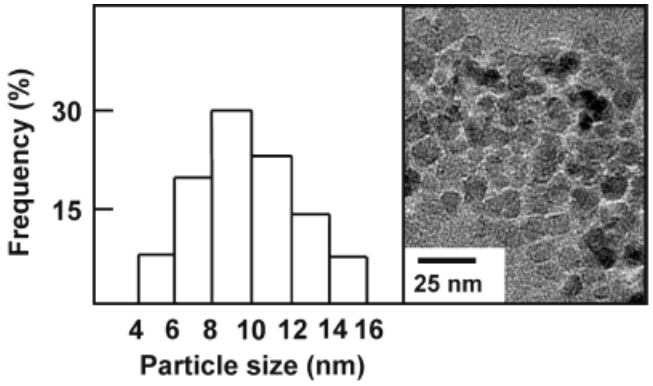

Fig. 1. Size histogram (left) and TEM image (right) of the surfactant-stabilized iron oxide nanoparticles.

The magnetization loop of the coated nanoparticles was measured at 10 K, Figure 2a. The magnetic nanoparticles exhibit hysteresis with a coercivity (150 G) and a remanent magnetization (13.2 emu/g) at 10 K, indicating the loss of superparamagnetism at this temperature. The temperature dependence of magnetization of the coated nanoparticles exhibits a cusp around 90 K in the zero-field-cooled (ZFC) susceptibility, and a blocking temperature T_B determined at the point where the ZFC and field-cooled (FC) curves merge, Figure 2b. Consistent with literature accounts,[17,18] below T_B, the thermal energy is not sufficient to overcome the magnetic anisotropy energy and magnetic interactions within the particles, and the superparamagnetism disappears.

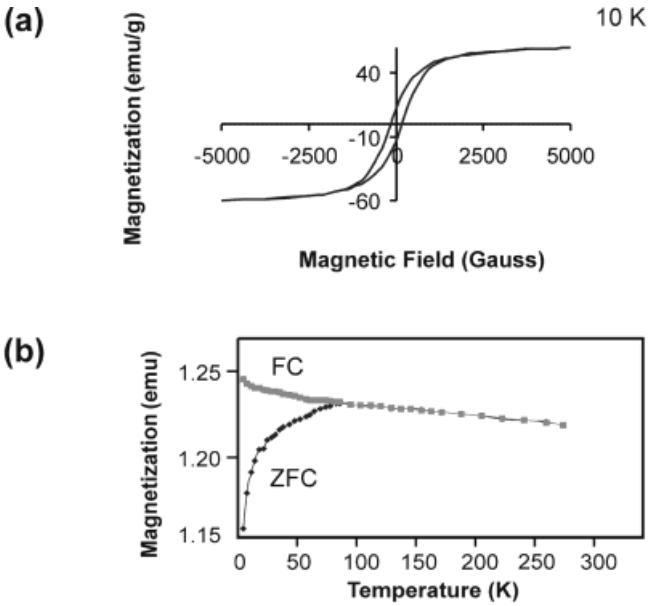

Fig. 2. Magnetization measurements of the coated iron oxide nanoparticles. a) Magnetization as a function of magnetic field. b) ZFC/FC curves.

In a typical patterning experiment, a silicon nitride tip was coated with MHA by dipping the entire cantilever into a saturated solution of MHA in acetonitrile for 30 s The cantilever was blown dry with compressed difluoroethane before being used. MHA patterns were generated on an Au substrate by bringing the tip in contact with the surface and traversing the tip over the surface in the form of the desired pattern, Scheme 1. The patterned Au substrates were then dipped into a saturated solution of 1-octadecanethiol (ODT) in acetonitrile for 30 s to form a passivating layer on the Au around the MHA nanostructures. After rinsing with acetonitrile and drying with compressed difluoroethane, the samples were dipped into a suspension of the iron oxide particles for 30 s and then dried under a flow of nitrogen overnight.[19] In a series of control experiments, which probed the importance of the basicity of the iron oxide solution, we confirmed that there was no

 © WILEY-VCH Verlag GmbH, D-69469 Weinheim, 2002 0935-9648/02/0302-0232 $ 17.50+.50/0

measurable effect on the resulting nanoparticle patterns over the pH 10–12.6 range. Finally, we observed that if one exceeded the specified concentration of the nanoparticle solutions, an increase in the thickness of the nanopatterns and non-specific particle binding often was observed.

With this strategy, magnetic dot- and line-features from 45 nm to many micrometers in length could be routinely generated, Figure 3a and b. The average height of each feature is 10 nm, consistent with monolayer formation. As expected, the size of the magnetic dots and lines generated in these experiments correlate with the size of the MHA dot and line templates. Significantly, the template dot diameter could be controlled by tuning the tip–substrate contact time, which exhibits the expected $t^{1/2}$ dependence,[12,13] Figure 3c, and the line width could be controlled by adjusting the scan speed, Figure 3d. These experiments demonstrate that one can use DPN to generate structures routinely on this length scale with precise control over feature size and shape.

Significantly, using this method we can generate arrays of nearly identical magnetic dots, Figure 4. In a typical experiment, an 8 × 8 square array of 75 nm MHA dots is generated via DPN and treated with the magnetic nanoparticles as described above. Topography AFM of the substrate shows that the iron oxide particles attach almost exclusively to the MHA template, generating iron oxide features of consistent size and shape (diameter = 75 ± 5 nm, height = 10 nm), Figure 4a–c. In an effort to demonstrate the generality of this approach, we also studied the assembly of magnetic nanoparticles (10 ± 5 nm) composed of manganese ferrite ($MnFe_2O_4$) using the procedure used for iron oxide.[20] Figure 5a shows magnetic dot- and line-nanostructures formed from the $MnFe_2O_4$ adsorbed onto an MHA template. Linewidth and dot size were intentionally changed (from 60 to 160 nm) to demonstrate the level of control this strategy offers. In addition, a 21 × 22 dot array of nanostructures was generated with a fixed dot diameter of 85 nm (±5) to demonstrate the reproducibility of the technique, Figure 5b.

In conclusion, we have presented a versatile new method for generating magnetic nanostructures with dimensions ranging from several hundred nanometers to sub-100 nm. In principle, this strategy could be extended to a wide variety of magnetic nanostructures comprised of different materials with precise control over feature size and shape as well as inter-feature distance. Significantly, this technique and the nanostructures generated by it point towards a straightforward route for studying the relationship between feature size, shape, and composition and inter-feature distance in nanomagnetics. Efforts in this direction are underway.

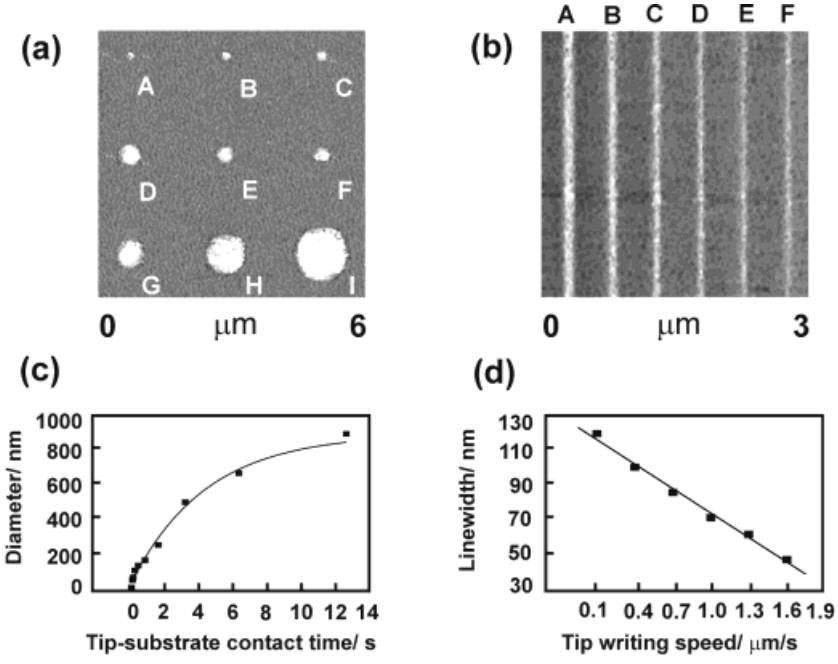

Fig. 3. Iron oxide nanostructures prepared according to Scheme 1. a) AFM topography image of magnetic structures formed on MHA dots generated via increasing tip–substrate contact times (A–I). The identification letter, time of MHA deposition, and measured diameter of the dots are the following: A: 0.05 s, 45 nm; B: 0.1 s, 60 nm; C: 0.2 s, 100 nm; D: 0.4 s, 130 nm; E: 0.8 s, 160 nm; F: 1.6 s, 250 nm; G: 3.2 s, 500 nm; H: 6.4 s, 670 nm; and I: 12.8 s, 920 nm. Image recorded at a scan rate of 1 Hz. b) AFM topography image of lines of magnetic nanostructures formed on lines of MHA generated at different tip writing speeds. The identification letter, speed of MHA deposition, and measured full width at half maximum (FWHM) of the magnetic lines are the following: A: 0.1 μm/s, 120 nm; B: 0.4 μm/s, 96 nm; C: 0.7 μm/s, 82 nm; D: 1.0 μm/s, 70 nm; E: 1.3 μm/s, 60 nm; F: 1.6 μm/s, 45 nm. Image recorded at a scan rate of 1 Hz. c) MHA dot diameter plotted as a function of deposition time. d) MHA linewidth plotted as a function of tip writing speed.

 © WILEY-VCH Verlag GmbH, D-69469 Weinheim, 2002 0935-9648/02/0302-0233 $ 17.50+.50/0

ADVANCED MATERIALS

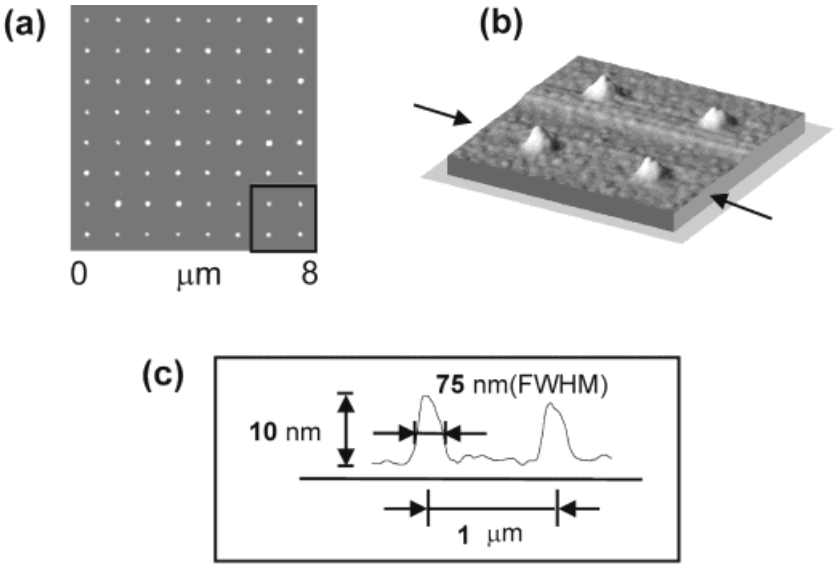

Fig. 4. An array of iron oxide dots prepared according to Scheme 1. a) AFM topography image of the dots. The MHA template used to assemble the magnetic nanostructures was fabricated with a tip–substrate contact time of 0.15 s. b) Three-dimensional topography image for a selected area (marked square) from Figure 4a. c) Cross-sectional topography trace of a line (marked by the arrows in (b)) through the centers of the dots.

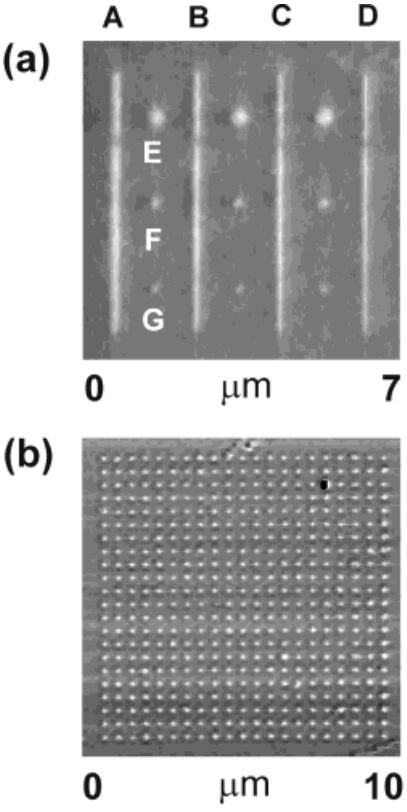

Fig. 5. Manganese ferrite nanostructures prepared according to Scheme 1. a) AFM topography image of the structures prepared on dots and lines of MHA, generated via various tip–substrate contact times or tip writing speeds. The identification letter, speed, or time of MHA deposition, and measured diameter of the dots or linewidth of the lines are the following: A: 0.06 μm/s, 160 nm; B: 0.08 μm/s, 140 nm; C: 0.1 μm/s, 120 nm; D: 0.8 μm/s, 75 nm; E: 1.4 s, 140 nm; F: 0.15 s, 80 nm; G: 0.1 s, 60 nm. Recorded at a scan rate of 1 Hz. b) AFM topography image of an array of the dots via a tip–substrate contact time of 0.18 s. Recorded at a scan rate of 1 Hz.

Experimental

The size and morphology of the surfactant stabilized iron oxide particles were determined with a HF-2000 field TEM (Hitachi, Japan). The size distribution was determined by measuring the diameters of 400 particles. Magnetic measurements were performed with a superconducting quantum interference device (SQUID) magnetometer (Quantum Design, MPMS). Blocking temperature (T_B) measurements were based on ZFC and FC (magnetization vs. temperature) curves with an external magnetic field of 1000 G. TGA measurements were taken using a TGA 2850 thermogravimetric analyzer (TA instruments) under N_2. The temperature range studied was from 30 to 700 °C at a rate of 5 °C/min. Au substrates were prepared by literature methods [12]. All DPN and imaging experiments were carried out with a Thermomicroscopes CP AFM and commercial cantilevers (Thermomicroscopes sharpened Microlever A, force constant = 0.05 N/m, Si_3N_4). To minimize piezo tube drift problems, a 100 μm scanner with closed loop scan control was used for all of the experiments. Typical ambient imaging conditions are 31 % humidity and 24 °C unless reported otherwise. Customized nanolithography software was utilized to make all array structures.

Received: August 16, 2001
Final version: November 6, 2001

[1] D. D. Awschalom, J. M. Kikkawa, *Phys. Today* **1999**, *52*, 33.
[2] G. A. Prinz, *Science* **1998**, *282*, 1660.
[3] H. Ohno, D. Chiba, F. Matsukura, T. Omiya, E. Abe, T. Dietl, Y. Ohno, K. Ohtani, *Nature* **2000**, *408*, 944.
[4] R. L. Edelstein, C. R. Tamanaha, P. E. Sheehan, M. M. Miller, D. R. Baselt, L. J. Whitman, R. J. Colton, *Biosens. Bioelectron.* **2000**, *14*, 805.
[5] M. S. Wei, S. Y. Chou, *J. Appl. Phys.* **1994**, *76*, 6679.
[6] Y. Xia, J. A. Rogers, K. Paul, G. M. Whitesides, *Chem. Rev.* **1999**, *99*, 1823.
[7] A. D. Kent, T. M. Shaw, S. von Molnár, D. D. Awschalom, *Science* **1993**, *262*, 1249.
[8] S. A. Gusev, N. A. Korotkova, D. B. Rozenstein, A. A. Fraerman, *J. Appl. Phys.* **1994**, *76*, 1994.
[9] R. D. Piner, J. Zhu, F. Xu, S. Hong, C. A. Mirkin, *Science* **1999**, *283*, 661.
[10] S. Hong, J. Zhu, C. A. Mirkin, *Science* **1999**, *286*, 523.
[11] S. Hong, C. A. Mirkin, *Science* **2000**, *288*, 1808.
[12] D. A. Weinberger, S. Hong, C. A. Mirkin, B. W. Wessels, T. B. Higgins, *Adv. Mater.* **2000**, *12*, 1600.
[13] A. Ivanisevic, C. A. Mirkin, *J. Am. Chem. Soc.* **2001**, *123*, 7887.
[14] L. M. Demers, C. A. Mirkin, *Angew. Chem. Int. Ed.* **2001**, *40*, 3069.
[15] L. M. Demers, S.-J. Park, T. A. Taton, Z. Li, C. A. Mirkin, *Angew. Chem. Int. Ed.* **2001**, *40*, 3071.
[16] L. Fu, V. P. Dravid, D. L. Johnson, *Appl. Surf. Sci.* **2001**, *181*, 173.
[17] T. Prozorov, R. Prozorov, A. Gedanken, *Adv. Mater.* **1998**, *10*, 1529.
[18] J. L. Dormann, D. Fiorani, *Magnetic Properties of Fine Particles*, North-Holland, Amsterdam **1992**.
[19] For patterning of magnetic materials on the micrometer scale, see: S. Palacin, P. C. Hidber, J.-P. Bourgoin, C. Miramond, C. Fermon, G. M. Whitesides, *Chem. Mater.* **1996**, *8*, 1316.
[20] Manganese ferrite nanoparticles were prepared according to a literature method: J. P. Chen, C. M. Sorensen, K. J. Klabunde, G. C. Hadjipanayis, E. Devlin, A. Kostikas, *Phys. Rev. B* **2001**, *54*, 9288.

 © WILEY-VCH Verlag GmbH, D-69469 Weinheim, 2002 0935-9648/02/0302-0234 $ 17.50+.50/0